Theoretical Models of the Ion Channel Structure of Amyloid β-Protein

Stewart R. Durell,* H. Robert Guy,* Nelson Arispe,‡ Eduardo Rojas,‡ and Harvey B. Pollard‡
*Laboratory of Mathematical Biology, National Cancer Institute, and ‡Lab of Cell Biology and Genetics, National Institutes of Diabetes and Digestive and Kidney Diseases, National Institutes of Health, Bethesda, Maryland 20892 USA

ABSTRACT Theoretical methods are used to develop models for the ion channel structure of the membrane-bound amyloid β-protein. This follows recent observations that the β-protein forms cation-selective channels in lipid bilayers in vitro. Amyloid β-protein is the main component of the extracellular plaques in the brain that are characteristic of Alzheimer's disease. Based on the amino acid sequence and the unique environment of the membrane, the secondary structure of the 40-residue β-protein is predicted to form a β-hairpin followed by a helix-turn-helix motif. The channel structures were designed as aggregates of peptide subunits in identical conformations. Three types of models were developed that are distinguished by whether the pore is formed by the β-hairpins, the middle helices, or by the more hydrophobic C-terminal helices. The latter two types can be converted back and forth by a simple conformational change, which would explain the variable conduction states observed for a single channel. It is also demonstrated how lipid headgroups could be incorporated into the pore lining, and thus affect the ion selectivity. The atomic-scale detail of the models make them useful for designing experiments to determine the real structure of the channel, and thus further the understanding of peptide channels in general. In addition, if β-protein-induced channel activity is found to be the cause of cell death in Alzheimer's disease, then the models may be helpful in designing counteracting drugs.

INTRODUCTION

The occurrence of Alzheimer's disease is associated with vascular and neuronal damage in the brain, involving the formation of intraneuronal neurofibrillary tangles and the accumulation of amyloid β-protein (AβP) in extracellular amyloid plaques (Blessed et al., 1968; Neve et al., 1990; Katzman and Saitoh, 1991; Selkoe, 1991; McKee et al., 1991; Hardy and Higgins, 1992; Kosik, 1992). Accordingly, it has been suggested that AβP is an important neurotoxic principle in the development of the disorder, and many experiments have been devoted to testing this hypothesis (Goldgaber et al., 1987; Tanzi et al., 1987; Joachim et al., 1988; Goate et al., 1991; Pike et al., 1991; Barger et al., 1993). Two concepts have emerged. The first is that AβP toxicity may be synergistic with other agents, such as with the excitatory amino acid glutamate (Koh et al., 1990; Mattson et al., 1992), or by the binding to tachykinin receptors (Yankner et al., 1990; Kimura and Schubert, 1993). The second, although not exclusive, possibility is that AβP is toxic by itself (Neve et al., 1990; Yankner et al., 1990), perhaps by raising the intracellular concentration of calcium ions (Joseph and Han, 1992). Consistent with the latter is our recent observation that AβP[1–40] forms "giant" cation-selective channels in lipid bilayers, with conduction values as large as 5 nS (Arispe et al., 1993a, b; Pollard et al., 1993).

Considerable effort has focused on determining the solution and solid-state structure of AβP and its fragments to better understand the extracellular plaques observed in vivo (Müller-Hill and Beyreuther, 1989; Kirschner et al., 1987; Halverson et al., 1990; Hilbich et al., 1991; Barrow and Zagorski, 1991; Barrow et al., 1992; Burdick et al., 1992; Inouye et al., 1993). In solution, AβP assumes different proportions of helix, β-sheet, and random coil and different degrees of aggregation depending on the environmental conditions. In the solid state, however, AβP is generally characterized by β-sheet structures. Unfortunately, the relevance of these data to the conformation of AβP in the membrane is not clear, because of the stratified hydrophilic/hydrophobic environment of the bilayer. Instead, we based our structure predictions on the amino acid sequence and its relation to patterns observed in other membrane-bound and channel-forming peptides and proteins. For example, the amphipathic pattern and turn sequence in the N-terminal region suggest that this part of the sequence forms a β-hairpin. Likewise, the hydrophobic character and transmembrane position of the C-terminal region of AβP in the precursor protein (Kang et al., 1987) suggest that this part of the sequence forms a membrane-embedded α-helix.

Previously, it has been demonstrated that similar ion channels are formed when AβP[1–40] is incorporated into artificial lipid bilayers by either the liposome fusion technique or directly from solution (Arispe et al., 1993a, b; Pollard et al., 1993). Single channels are observed to convert within and between two conduction ranges: 40–400 pS and 0.4–5.0 nS. Both of these "large" and "giant" sized channels are cation-selective; however, the "giant" channel is considerably less susceptible to blockage by tromethamine. Because of the suspected large physical size of the channel structures, the models were designed as aggregates of many membrane-bound AβP subunits. The process used to develop the models is an extension of our work with other channel forming peptides, which includes cecropin, magainin, δ-hemolysin, and pardaxin (Durell et al., 1992; Cruciani et al., 1992; Raghunathan et al., 1990; Lazarovici et al., 1992) and is a combination of theoretical principles with experimental data on the conductance of the channel.

Three basic types of channel models were developed. These are distinguished by whether the pore is formed by a β-barrel (comprised of the N-terminal β-hairpins) or by a grouping of the middle and/or C-terminal helices. The latter two channel types are interconvertible by a simple conformational change. This alters the proportions of the pore and thus could explain the observed "spontaneous" conduction changes. To examine the

possible modes of peptide-membrane binding and channel formation, some models were developed with lipid molecules incorporated into the structures. In this case, the specific conformations and identities of the lipid headgroups would affect the properties of the pore. It is hoped that the ideas embodied in these models will prove useful in designing tests of AβP and other peptide channel structures. The coordinates are available from the corresponding authors upon request.

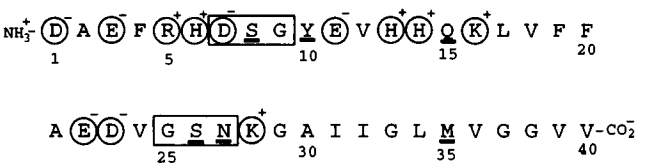

FIGURE 1 Amino acid sequence of AβP[1–40]. The circles indicate the charged residues, the underscores indicate the polar-neutral residues, and the remaining residues are considered hydrophobic. The rectangles indicate predicted turn regions.

MATERIALS AND METHODS

Because current methods cannot calculate accurately the free energy of the ion channel models, which would include interactions between the peptides, lipids, solvent, and ions, a number of principles are used to construct structures that are expected to be thermodynamically stable. The main principle requires positioning the polar and nonpolar amino acid residues in either hydrophilic or hydrophobic environments, respectively. For the polar residues, this means limiting contact to other polar residues, the lipid headgroups, and/or the solvent. This also results in maximizing the number of stabilizing hydrogen bonds and salt-bridges. Likewise, the nonpolar residues are limited to contact with other nonpolar residues and/or the alkyl chains of the lipids. A second principle concerns the packing of the peptide subunits, such that unrealistic atomic overlaps and internal cavities are avoided. This is achieved by optimizing the van der Waals energy.

The first assumption used in designing the models was that the channels are formed from an assembly of AβP[1–40] subunits. Otherwise, it is hard to imagine how a single AβP molecule, which is not quite long enough to form two transmembrane helices, could form a channel structure responsible for such large observed conductances (up to 5 nS). A second assumption was that each subunit assumes the same conformation and that they are arranged symmetrically around the axis of the pore. Although not unexpected on energetic grounds, this restriction also simplifies the modeling procedure by reducing the number of possible inter-subunit arrangements.

Once a basic structural motif was devised and built on the computer, an iterative procedure of direct manipulation and automated energy minimization was used to refine the models in accord with the principles described above. In particular, the Quanta computer program (Molecular Simulations, Inc., Waltham, MA) was used to adjust the torsional angles into the desired backbone and side-chain conformations, and the Minimization facility of the CHARMM computer program (Brooks et al., 1983; Molecular Simulations) was used to optimize the packing for that specific conformation (which includes removing atomic overlap and tuning the salt-bridges and hydrogen bonds). The minimization procedure typically consisted of 100 steps of Steepest Descent followed by 300 steps of Adopted Basis Newton-Raphson, utilizing the residue topology and PARM30 parameters provided with the commercial version of CHARMM. The Image facility was used for the minimization of multimeric channel structures. It must be emphasized that the purpose of the automated energy minimization was simply to optimize the packing within the local minimum associated with the starting conformation. No attempt was made to search for the "correct" conformation of the protein with minimization and/or dynamics procedures, which would require accurately representing the membrane and solvent environments and sufficiently sampling the extremely large conformational space. For this reason, only a simple distance-dependent dielectric constant was used for the electrostatic interactions.

The concepts for the channel structure assemblies were developed from the particular arrangement of secondary structure elements that we predicted for AβP[1–40] in a membrane/solvent environment, which is described below. The sequence of AβP used in the channel measurements is shown in Fig. 1. Except for the histidines, the circles indicate those residues that would be formally charged at the experimental conditions of pH 7.0 and 7.4 (Arispe et al., 1993a, b; Pollard et al., 1993). Because this is only slightly above the intrinsic pK_a of the peptide-bound imidazole ring (~6.5–7.0), the actual charged states of the histidines would be strongly influenced by the local environment. The underscores indicate the polar-neutral residues. The remaining residues are considered hydrophobic.

As pointed out by Kirschner et al. (1987), there are two regions within the first 28 residues of the sequence that have a high propensity for producing a turn in the 3-D structure (Chou and Fasman, 1978). These are indicated by rectangular boxes in Fig. 1. The next most striking feature is that the first turn segment is flanked on both sides by a short stretch of alternating charged and hydrophobic residues. For a peptide bound in the mixed hydrophilic/hydrophobic environment of a membrane, this type of amphipathic pattern suggests that the first 13 residues of the sequence form a β-hairpin structure. The three-residue linker of the hairpin would likely form some type of γ-turn structure (Sibanda et al., 1989; Rose et al., 1985). After the second turn segment (second rectangle), the remaining residues [28–40] are mostly nonpolar and are thus likely to be embedded in the hydrophobic core of the membrane. In this case, and despite the extra-flexible glycines, the sequence would likely adopt a helical conformation to form hydrogen bonds and thus reduce the destabilizing effect of the peptide backbone partial charges. It should be pointed out, however, that a circular dichroism analysis of the AβP[29–42] fragment in reduced polarity solvent failed to detect appreciable amounts of helical secondary structure (Barrow et al., 1992). However, the hydroxyl-group-containing trifluoroethanol and hexafluoro-2-propanol solvents used in that study are still more polar than the alkyl-chain core of a membrane. Furthermore, this C-terminal region of AβP has been identified as forming the outer half of the single transmembrane domain of the amyloid precursor protein (Kang et al., 1987), which would generally be believed to have a helical conformation. The prediction for this region also corresponds with the occurrence of an asparagine at position 27, which is the most commonly observed residue found at the N-terminal cap of helices in known protein structures (Richardson and Richardson, 1988). Another interesting feature is that in a helical conformation the four glycine residues at positions 29, 33, 37, and 38 would result in an exposed band along one side of the helix. Finally, residues 16–24 were postulated to form a second helix, which is in the middle of the sequence. This was based on the Chou-Fasman prediction values (Chou and Fassman, 1978) and the general observation that hydrophobic segments form helices in membranes. In addition, the glycine at position 25, in the second turn region, corresponds with the fact that this is the most likely type of residue to terminate a helix in known protein structures (Richardson and Richardson, 1988).

RESULTS

As described in Materials and Methods, Fig. 2 shows the basic secondary structure predicted for a membrane-bound AβP[1–40] molecule. The blue and red letters indicate the positive and negatively charged residues, respectively. As can be seen from the alternating pattern, the β-hairpin structure would be amphipathic, with the hydrophilic E3, R5, E11, and H13 residues projecting from one side, and the hydrophobic A2, F4, Y10, and V12 residues projecting from the other side. Following a small linker is the relatively short middle helix. Although hydrophobic in the center, this helix has a positively charged residue (K16) at the N-terminal end and two negatively charged residues (E22 and D23) at the C-terminal end. Finally, the N27 residue forms

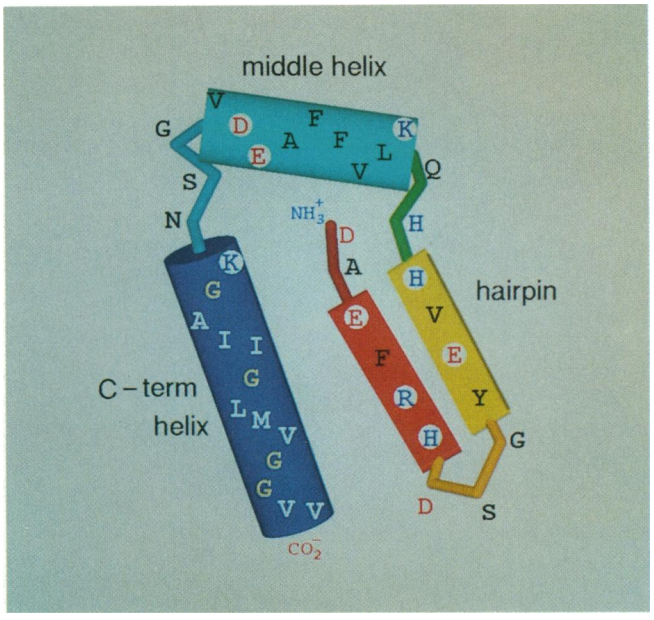

FIGURE 2 Secondary structure prediction for a membrane-bound AβP molecule. The red and yellow rectangles indicate the β-strands of the hairpin, and the large cyan and blue cylinders indicate the middle and C-terminal helices, respectively. The blue and red letters indicate the positive and negatively charged residues, respectively. The four glycines in the C-terminal helix are highlighted in yellow. (Although not clear in the figure, the second half of the A2 residue is actually part of the β-hairpin structure.)

the N-terminal cap of the more hydrophobic C-terminal helix, which comprises the remainder of the sequence. As also seen in the figure, the four glycine residues (G29, 33, 37, and 38) are stacked above each other. Because these residues are devoid of side chains, they expose the backbone atoms along one side of the helix.

Type I models

Fig. 3 shows schematic side and top views of a parallel Type I channel formed from six identical AβP subunits, as it would be embedded in a membrane. The red and yellow rectangles indicate the β-strands, the cyan cylinders indicate the middle helices, and the blue cylinders indicate the C-terminal helices. This is described as a parallel structure because each subunit is oriented in the same direction. The pore is formed by the 6 β-hairpins, which results in a 12-stranded, antiparallel β-barrel. The lining of the pore is formed from the charged and polar-neutral D1 (including the $(NH_3)^+$ group), E3, R5, D7, S8, E11, H13, and H14 residues, which form salt-bridge and hydrogen bond networks. If not all the histidines are protonated, which is likely at the experimental conditions of pH 7.0 (Arispe et al., 1993b) and 7.4 (Arispe et al., 1993a), then the pore would have a net negative charge. This would explain the cation selectivity of the channels observed in vitro (Arispe et al., 1993a, b; Pollard et al., 1993). Above the pore are the six middle helices arranged in a circle, parallel to the membrane plane. Because they contain both charged and nonpolar residues, they are embedded in the top headgroup layer of the membrane where both hydrophilic and hydrophobic contacts can be made. The head-to-tail arrangement stabilizes the aggregate channel structure by forming complementary electrostatic interactions between the dipolar ends. In addition, each K16 residue forms a stabilizing salt-bridge with the D23 residue of the adjacent subunit, and each E22 residue forms a salt-bridge with the K28 residue of the same subunit (not shown). Finally, the pore is surrounded by the six hydrophobic C-terminal helices, which transverse the membrane core. Although not providing a complete barrier, these helices serve to anchor and shield the pore from the disruptive motions of the lipids.

As shown in Fig. 4, an antiparallel version of the Type I channel can be formed from 12 identical AβP subunits. The structure can be thought of as two 6-subunit parallel channels (Fig. 3) arranged tail-to-tail. The pore is formed by the two 12-stranded antiparallel β-barrels arranged in tandem. The middle helices, which are embedded in the headgroup layers, form stabilizing 6-membered rings on both sides of the membrane. The pore is surrounded by the 12 hydrophobic C-terminal helices, which are interlaced in an antiparallel fashion. This provides a denser barrier between the pore and the lipids than in the parallel model. Also, in contrast, the antiparallel channel provides a symmetric profile for the conduction of ions across the membrane.

In these models, the size of the pore is determined by the number of AβP subunits incorporated into the complex. In Fig.3, the minimum radius of the 6-subunit parallel Type I channel is 2.7 Å. However, the actual width of the pore may differ because of interactions with the solvent. A similar channel built with only four AβP subunits was found to have a minimum pore radius of 1.4 Å (not shown). Because the channels with the smallest conduction were able to pass cations as large as Cs^+ (Arispe et al., 1993b), which has an ionic radius of ~1.7 Å, it would seem that four or five AβP subunits is the minimum number required to form an active, parallel Type I channel. However, we suspect that a 4-subunit, 8-stranded β-barrel pore would be too small to accommodate the large number of charged residues in the lining. Larger pores are favored because they allow for more water molecules to solvate the charges. The channels were also found to be blocked reversibly by tromethamine and irreversibly by Al^{3+} (Arispe et al., 1993a, b; Pollard et al., 1993). The action of tromethamine is understandable considering its relatively large size in relation to the pore width. However, the blocking action of Al^{3+}, which has a relatively small ionic radius (~0.5 Å) is more difficult to interpret. One possibility is that the high charge density causes one or more of these ions to bind tightly to the negatively charged residues of the pore lining (i.e., D1, E3, D7, or E11).

Type II and III models

Fig. 5 displays schematic side and top views of the type II channel formed from four AβP subunits. In this model, the pore is in the shape of a funnel, with the "cone" formed by the middle helices (*cyan cylinders*) and lipid headgroups (*dark gray spheres*) and the "spout" formed by the long C-terminal helices (*blue cylinders*). The C-terminal helices are oriented such that the glycine-containing faces (see Fig. 2) are toward the center.

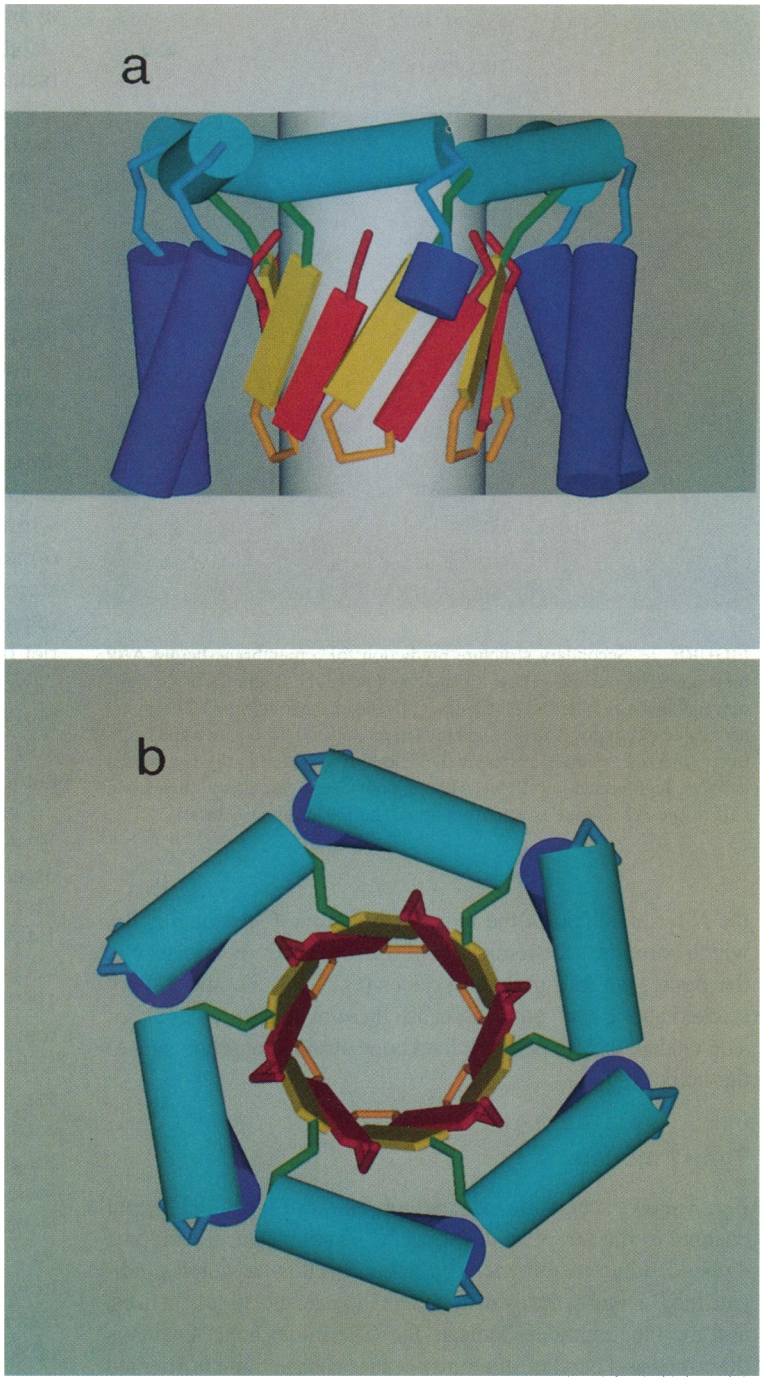

FIGURE 3 Schematic side (*a*) and top (*b*) views of the parallel Type I channel. The color code is the same as in Fig. 2. The front C-terminal helix in the side view was truncated to expose the β-barrel.

Because glycine residues lack bulky side chains, the helices are able to pack closely while maintaining a reasonably sized pore radius (~2.5Å). In addition, the lack of a side chain exposes the partial negatively charged carbonyl oxygen atoms of the peptide backbone. Although not in the same β(L,D)-helix conformation (Nicholson and Cross et al., 1989), this provides a cation-selective environment similar to gramicidin A (Gennis, 1989). Because the middle helices are at a 45° angle to the membrane plane, Fig. 5 also shows how the charged phosphatidylserine lipid headgroups (*dark gray spheres*) would naturally fall into the four wedge-shaped spaces between them. This association is stabilized by salt-bridges with the positively and negatively charged K16, E22, and D23 residues. In this way, the charged headgroups become part of the pore lining, where they would affect the ion selectivity of the channel. Finally, the hydrophobic sides of the four amphipathic β-hairpins are used to cover the alkyl chains of the channel-incorporated lipids, which would otherwise be exposed to solvent because of their nonperpendicular orientation with respect to the membrane plane.

The Type III channel is shown in Fig. 6. As seen from the 2-subunit side views in Fig. 7, the Type III channel is formed from a concerted conformational change of the Type II channel, in which the hydrophobic C-terminal helices (*blue cylinders*) move from a transmembrane orientation to a parallel

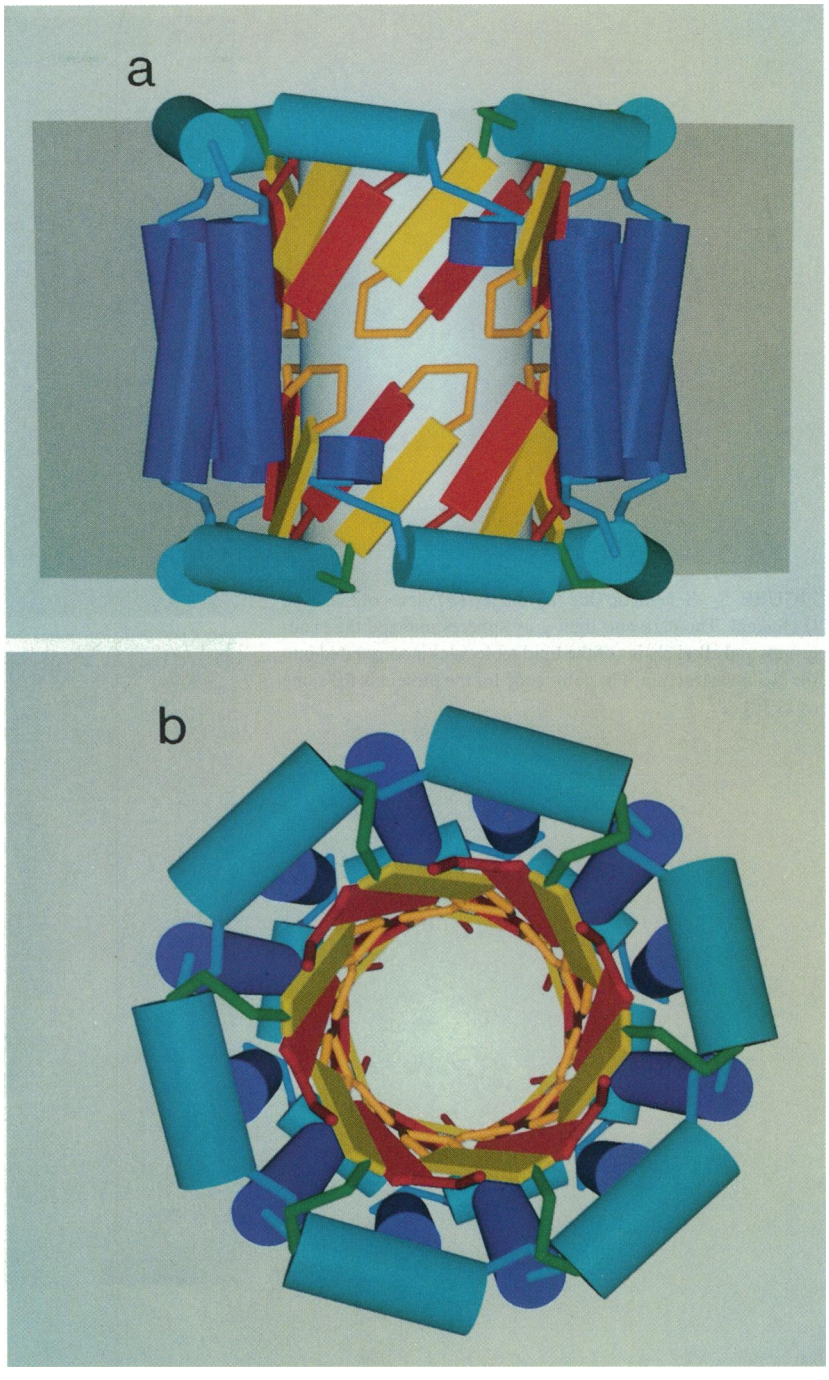

FIGURE 4 Schematic side (*a*) and top (*b*) views of the antiparallel Type I channel. The color code is the same as in Fig. 2. The front C-terminal helices in the side view were truncated to expose the tandem β-barrels.

position in the bottom alkyl-chain layer of the membrane. The helices are oriented such that the semi-hydrophilic, glycine-containing edge, which formed the lining of the pore in the Type II model, is at the mixed polarity alkyl-chain/headgroup interface. In the Type III channels, the pore is formed exclusively by the four middle helices (*cyan cylinders*) and the lipid headgroups (*dark gray spheres*) that were bound in the Type II model (see Fig. 5). For the specific structure shown in Fig. 6, the minimum radius of the pore is 3.0 Å. However, larger or smaller sizes could easily result from small adjustments of the peptide/lipid interactions. As also shown in Fig. 6, the alkyl-chains of the incorporated lipids (*light gray spheres*), which are parallel to the membrane plane, are shielded by the amphipathic β-hairpins on the top side of the membrane and by the hydrophobic residues of the C-terminal helices on the bottom side.

DISCUSSION

Our procedures have resulted in three basic types of AβP channel models, which are distinguished by the orientation of the subunits in the membrane, and thus the portion of the amino acid sequence that forms the pore lining. Although the

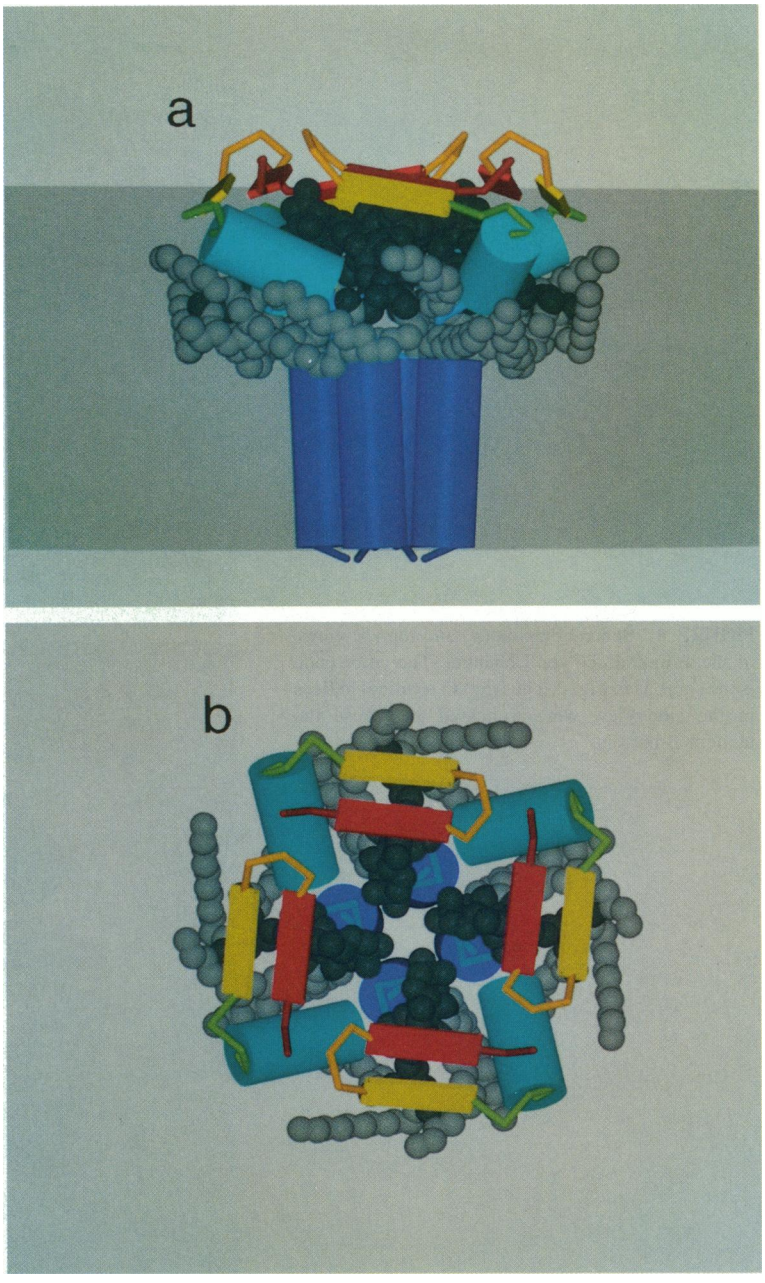

FIGURE 5 Schematic side (*a*) and top (*b*) views of the Type II channel. The dark and light gray spheres indicate the headgroups and alkyl chains of the lipid molecules incorporated into the channel structure. The color code for the protein is the same as in Fig. 2.

models were computer-built at the atomic scale, they should only be considered as representative of basic structural motifs. For instance, for any specific assembly pattern, it is usually possible to rearrange the side-chain conformations and thus form different networks of salt-bridges and hydrogen bonds. This is especially true for the incorporated lipid molecules, which have many degrees of freedom

Experimentally, it has been demonstrated that active channels can be formed when AβP[1–40] is incorporated into the bilayer by either the liposome fusion technique or directly from solution (Arispe et al., 1993a, b; Pollard et al., 1993). We envision two basic mechanisms by which the AβP molecules would bind to the membrane and rearrange to form the channel structures. In the first mechanism, the AβP molecules would initially bind to one side of the membrane and diffuse to form a 2-D lattice, or raft-like structure, on the surface. The amphipathic "raft" would be embedded in the headgroup layer of the membrane such that the nonpolar residues would be in contact with the alkyl chains at the bottom, and the polar residues would be in contact with the lipid headgroups and solvent at the top. It is then imagined that the "raft" structure would fold in half such that the middle section would be pushed through to the opposite side of the membrane. Concurrently, both sides would curve around the transmembrane axis to form a cylindrical, Type I channel (Figs. 3 and 4). By this concerted conformational change, the charged residues of the β-hairpins move from the top side of the membrane to the lining of the pore without having to be exposed to the

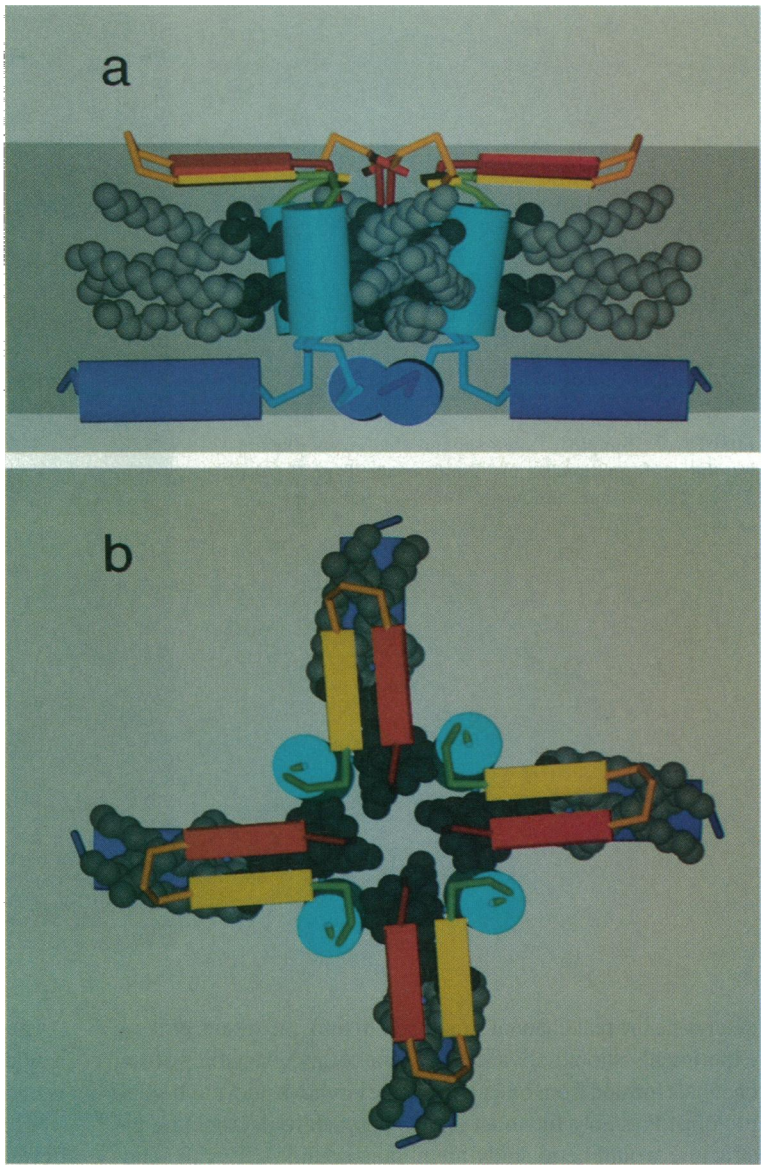

FIGURE 6 Schematic side (*a*) and top (*b*) views of the Type III channel. The color code is the same as in Fig. 5.

hydrophobic alkyl-chains of the lipids, which would be energetically disfavored. Whether a parallel or antiparallel Type I channel is formed would depend on the symmetry of the initial lattice structure. A similar raft insertion mechanism was illustrated for the δ-hemolysin peptides (Raghunathan et al., 1990).

The second mechanism assumes that each AβP molecule has inserted individually into the membrane, with the amphipathic β-hairpin and middle helix in the headgroup layer and the hydrophobic C-terminal helix in a transmembrane position. The next step would be the association of four or more subunits into a ring, excluding lipid molecules from the center. At this stage, the formation of the parallel Type I and Type II channels are both possible. A Type I channel would result simply from the β-hairpins folding into the center of the ring and forming the β-barrel pore. Similarly, the Type II channel would result form the transmembrane C-terminal helices packing with their glycine-containing sides oriented toward the center. As discussed above, a Type III channel could then be formed from a concerted conformational change of the Type II channel (see Fig. 7).

It has also been observed experimentally that a single AβP channel can undergo transitions between a number of different conduction states in the pico- ("large") and nanosiemens ("giant") ranges (Arispe et al., 1993a, b; Pollard et al., 1993). One possible explanation is that this is because of conversions between the Type II and Type III channel structures, which have different intrinsic pore sizes. In addition, the exact size of the pore would be affected by random variations in the protein and lipid binding conformations after each transition. An alternative explanation, which also includes the Type I channels, is that the change in pore size is caused by the rapid incorporation or elimination of AβP subunits. This could happen on a single subunit basis or by the coalescence or separation of two multisubunit channel structures.

The channel models presented here are useful because they explore a number of possibilities and suggest experiments to

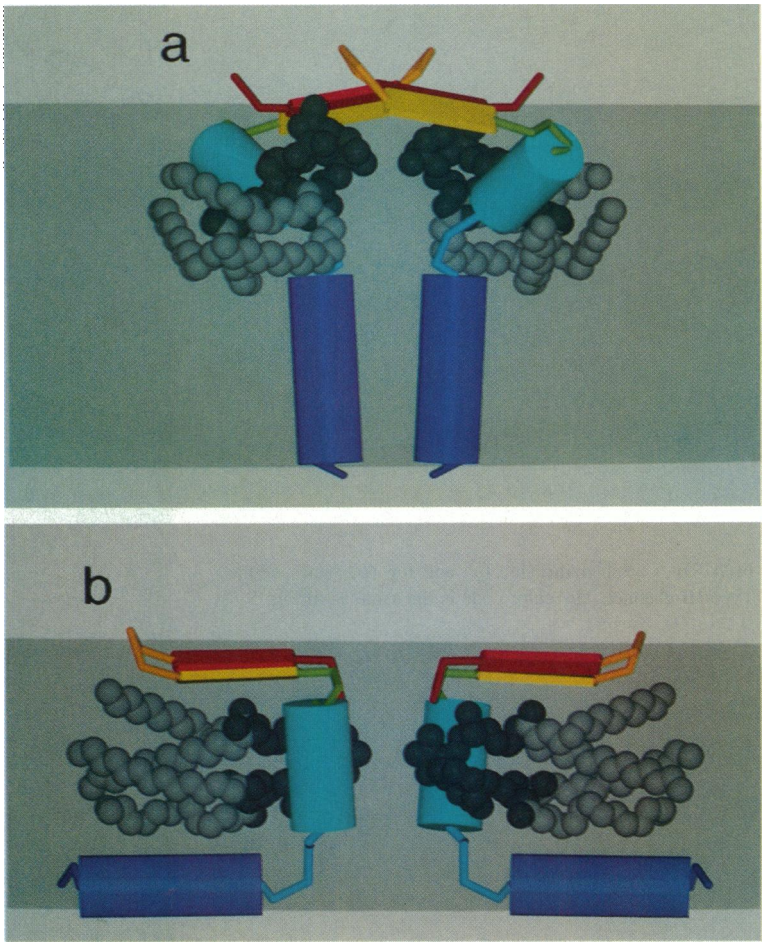

FIGURE 7 Simplified, two-subunit side views illustrating the conformational transition from the Type II (*a*) to Type III (*b*) channel structures. The color code is the same as in Fig. 2.

determine the real channel structures. In turn, the results of these experiments should advance the general understanding of ion channels formed from other membrane bound peptides and small proteins. Probably the most direct approach to determining the structure would be to study membrane-bound AβP with solid-state NMR and/or electron cryo-microscopy methods. Failing these, a less direct approach would be to examine the effects of sequence mutations and changes in environmental conditions on the properties of the channels. For example, the presence of the Type I motif could be verified by examining the effects of amino acid substitutions in the β-hairpin region of the sequence. One possible experiment would be to neutralize the negative electrostatic charge of the D1, E3, D7, and/or E11 residues by substitution to either asparagine or glutamine, as appropriate. If the pore of the channel is indeed formed by the β-hairpins, then this type of mutation would either reduce or eliminate the cation selectivity. Likewise, a similar effect should be observed by lowering the solution pH below the pK_a of the histidine residues, which would effectively neutralize the net charge of the putative β-barrel pore. On the other hand, these perturbations would have little or no effect on the conduction properties of Type II or III channels, where the pore is formed by the middle and/or C-terminal helices. If the results point to the Type I motif, then the parallel or antiparallel type structure could be distinguished by determining whether the conduction and drug binding properties are symmetric with respect to both sides of the membrane. As mentioned in Results, the antiparallel Type I model provides a symmetric profile across the membrane, whereas the parallel version does not.

Previously, we have discussed the possible connection between the "giant" nanosiemens (nS) conductance of the AβP[1–40] channels observed in artificial bilayers with the death of neurons in Alzheimer's disease (Arispe et al., 1993a, b; Pollard et al., 1993). This view is supported by the fact that AβP added to neuron tissue culture has been observed to disrupt $[Ca^{2+}]_i$ homeostasis (Joseph and Han, 1992; Barger et al., 1993), which itself has been associated with cell death (Hardy and Higgins, 1992; Mattson et al., 1992; Kimura and Schubert, 1993). If this theory proves true, then the ion channel models would be useful for designing inhibitory drugs.

REFERENCES

Arispe, N., H. B. Pollard, and E. Rojas. 1993a. Giant multilevel cation channels formed by Alzheimer disease amyloid β-protein [AβP-(1–40)] in bilayer membranes. *Proc. Natl. Acad. Sci. USA.* 90:10573–10577.

Arispe, N., E. Rojas, and H. B. Pollard. 1993b. Alzheimer disease amyloid β protein forms calcium channels in bilayer membranes: blockade by tromethamine and aluminum. *Proc. Natl. Acad. Sci USA.* 90: 567–571.

Barger, S. W., V. L. Smith-Swintosky, R. E. Rydel, and M. P. Mattson. 1993. β-Amyloid precursor protein mismetabolism and loss of calcium homeostasis in Alzheimer's disease. *Ann N. Y. Acad. Sci.* 695:158–164.

Barrow, C. J., A. Yasuda, P. T. M. Kenny, and M. G. Zagorski. 1992. Solution conformations and aggregational properties of synthetic amyloid β-peptides of Alzheimer's disease. *J. Mol. Biol.* 225:1075–1093.

Barrow, C. J., and M. G. Zagorski. 1991. Solution structures of β peptide and its constituent fragments: Relation to amyloid deposition. *Science.* 253:179–182.

Blessed, G., B. E. Tomlinson, and M. Roth. 1968. The association between quantitative measures of dementia and of senile change in the cerebral grey matter of elderly subjects. *Br. J. Psychiatry.* 114:797–811.

Brooks, B. R., R. E. Bruccoleri, B. D. Olafson, D. J. States, S. Swaminathan, and M. Karplus. 1983. CHARMM: A program for macromolecular energy, minimization, and dynamics calculations. *J. Comp. Chem.* 4:187–217.

Burdick, D., B. Soreghan, M. Kwon, J. Kosmoski, M. Knauer, A. Henschen, J. Yates, C. Cotman, and C. Glabe. 1992. Assembly and aggregation properties of synthetic Alzheimer's A4/β amyloid peptide analogs. *J. Biol. Chem.* 267:546–554.

Chou, P. Y., and G. D. Fasman. 1978. Empirical predictions of protein conformation. *Ann. Rev. Biochem.* 47:251–276.

Cruciani, R. A., J. L. Barker, S. R. Durell, G. Raghunathan, H. R. Guy, M. Zasloff, and E. F. Stanley. 1992. Magainin 2, a natural antibiotic from frog skin, forms ion channels in lipid bilayer membranes. *Eur. J. Pharmacol.* 226:287–296.

Durell, S. R., G. Raghunathan, and H. R. Guy. 1992. Modeling the ion channel structure of cecropin. *Biophys. J.* 63:1623–1631.

Gennis, R. B. 1989. Biomembranes: Molecular Structure and Function. Springer-Verlag, New York. 288–290.

Goate, A., M.-C. Chartier-Harlin, M. Mullan, J. Brown, F. Crawford, L. Fidani, L. Giuffra, A. Haynes, N. Irving, L. James, R. Mant, P. Newton, K. Rooke, P. Roques, C. Talbot, M. Pericak-Vance, A. Roses, R. Williamson, M. Rossor, M. Owen, and J. Hardy. 1991. Segregation of a missense mutation in the amyloid precursor protein gene with familial Alzheimer's disease. *Nature.* 349:704–706.

Goldgaber, D., M. I. Lerman, O. W. McBride, U. Saffiotti, and D. C. Gajdusek. 1987. Characterization and chromosomal localization of a cDNA encoding brain amyloid of Alzheimer's disease. *Science.* 235:877–880.

Halverson, K., P. E. Fraser, D. A. Kirschner, and P. T. Lansbury, Jr. 1990. Molecular determinants of amyloid deposition in Alzheimer's disease: conformational studies of synthetic β-protein fragments. *Biochemistry.* 29:2639–2644.

Hardy, J. A., and G. A. Higgins. 1992. Alzheimer's disease: the amyloid cascade hypothesis. *Science.* 256:184–185.

Hilbich, C., B. Kisters-Woike, J. Reed, C. L. Masters, and K. Beyreuther. 1991. Aggregation and secondary structure of synthetic amyloid βA4 peptides of Alzheimer's disease. *J. Mol. Biol.* 218:149–163.

Inouye, H., P. E. Fraser, and D. A. Kirschner. 1993. Structure of β-crystallite assemblies formed by Alzheimer β-amyloid protein analogues: analysis by x-ray diffraction. *Biophys. J.* 64:502–519.

Joachim, C. L., L. K. Duffy, J. H. Morris, and D. J. Selkoe. 1988. Protein chemical and immunocytochemical studies of meningovascular β-amyloid protein in Alzheimer's disease and normal aging. *Brain Res.* 474:100–111.

Joseph, R., and E. Han. 1992. Amyloid β-protein fragment 25–35 causes activation of cytoplasmic calcium in neurons. *Biochem. Biophys. Res. Commun.* 184:1441–1447.

Kang, J., H.-G. Lemaire, A. Unterbeck, J. M. Salbaum, C. L. Masters, K.-H. Grzeschik, G. Multhaup, K. Beyreuther, and B. Müller-Hill. 1987. The precursor of Alzheimer's disease amyloid A4 protein resembles a cell-surface receptor. *Nature.* 325:733–736.

Katzman, R., and T. Saitoh. 1991. Advances in Alzheimer's disease. *FASEB J.* 5:278–286.

Kimura, H., and D. Schubert. 1993. Amyloid β-protein activates tachykinin receptors and inositol trisphosphate accumulation by synergy with glutamate. *Proc. Natl. Acad. Sci. USA.* 90:7508–7512.

Kirschner, D. A., H. Inouye, L. K. Duffy, A. Sinclair, M. Lind, and D. J. Selkoe. 1987. Synthetic peptide homologous to β protein from Alzheimer disease forms amyloid-like fibrils in vitro. *Proc. Natl. Acad. Sci. USA.* 84:6953–6957.

Koh, J.-Y., L. L. Yang, and C. W. Cotman. 1990. β-amyloid protein increases the vulnerability of cultured cortical neurons to excitotoxic damage. *Brain Res.* 533:315–320.

Kosik, K. S. 1992. Alzheimer's disease: a cell biological perspective. *Science.* 256:780–783.

Lazarovici, P., C. Edwards, G. Raghunathan, and H. R. Guy. 1992. Secondary structure, permeability and molecular modeling of pardaxin pores. *J. Natural Toxins.* 1:1–15.

Mattson, M. P., B. Cheng, D. Davis, K. Bryant, I. Lieberburg, and R. E. Rydel. 1992. β-amyloid peptides destabilize calcium homeostasis and render human cortical neurons vulnerable to excitotoxicity. *J. Neurosci.* 12:376–389.

McKee, A. C., K. S. Kosik, and N. W. Kowall. 1991. Neuritic pathology and dementia in Alzheimer's disease. *Ann. Neurol.* 30:156–165.

Müller-Hill, B., and K. Beyreuther. 1989. Molecular biology of Alzheimer's disease. *Annu. Rev. Biochem.* 58:287–307.

Neve, R. L., L. R. Dawes, B. A. Yankner, L. I. Benowitz, W. Rodriguez, and G. A. Higgins. 1990. Genetics and biology of the Alzheimer amyloid precursor. *Prog. Brain Res.* 86:257–267.

Nicholson, L. K., and T. A. Cross. 1989. Gramicidin cation channel: an experimental determination of the right-handed helix sense and verification of β-type hydrogen bonding. *Biochemistry.* 28:9379–9385.

Pike, C. J., A. J. Walencewicz, C. G. Glabe, and C. W. Cotman. 1991. In vitro aging of β-amyloid protein causes peptide aggregation and neurotoxicity. *Brain Res.* 563:311–314.

Pollard, H. B., E. Rojas, and N. Arispe. 1993. A new hypothesis for the mechanism of amyloid toxicity, based on the calcium channel activity of amyloid β protein (AβP) in phospholipid bilayer membranes. *Ann. N. Y. Acad. Sci.* 695:165–168.

Raghunathan, G., P. Seetharamulu, B. R. Brooks, and H. R. Guy. 1990. Models of δ-hemolysin membrane channels and crystal structures. *Proteins Struct. Funct. Genet.* 8:213–225.

Richardson, J. S., and D. C. Richardson. 1988. Amino acid preferences for specific locations at the ends of α helices. *Science.* 240:1648–1652.

Rose, G. D., L. M. Gierasch, and J. A. Smith. 1985. Turns in peptides and proteins. *Adv. Protein Chem.* 37:1–109.

Selkoe, D. J. 1991. The molecular pathology of Alzheimer's disease. *Neuron.* 6:487–498.

Sibanda, B. L., T. L. Blundell, and J. M. Thornton. 1989. Conformation of β-hairpins in protein structures: a systematic classification with applications to modelling by homology, electron density fitting and protein engineering. *J. Mol. Biol.* 206:759–777.

Tanzi, R. E., J. F. Gusella, P. C. Watkins, G. A. P. Bruns, P. St. George-Hyslop, M. L. Van Keuren, D. Patterson, S. Pagan, D. M. Kurnit, and R. L. Neve. 1987. Amyloid β protein gene: cDNA, mRNA distribution, and genetic linkage near the Alzheimer locus. *Science.* 235:880–884.

Yankner, B. A., L. K. Duffy, and D. A. Kirschner. 1990. Neurotrophic and neurotoxic effects of amyloid β protein: reversal by tachykinin neuropeptides. *Science.* 250:279–282.